PERGAMON

International Journal of Heat and Mass Transfer 44 (2001) 1259–1266

International Journal of
HEAT and MASS TRANSFER

www.elsevier.com/locate/ijhmt

The effect of non-absorbable gas on an absorption process for the falling film flow inside a porous medium

Ru Yang [a,*], Te-Ming Jou [b]

[a] *Department of Mechanical Engineering, National Sun Yat-Sen University, Kaohsiung 804, Taiwan, ROC*
[b] *Department of Mechanical Engineering, Far East College, Tainan, Taiwan, ROC*

Received 20 October 1999

Abstract

The effect of non-absorbable gas on the heat and mass transfer for an absorption process taking place on a falling film flow in a porous medium is studied numerically. The liquid flow is modeled by the Brinkman–Forchhiemer extended Darcy equation. The solutions show that the non-absorbable gas has a strong effect in reducing mass absorption rate. The mass absorption rate increases with increasing solution flow rate, conductivity ratio and absorber pressure, and decreases with increasing porosity and the concentration of non-absorbable gas. An optimum conductivity ratio of 10 is observed while a minimum porosity of 0.9 is obtained. © 2001 Elsevier Science Ltd. All rights reserved.

Keywords: Non-absorbable gas; Falling film absorption; Porous medium

1. Introduction

Gas absorption into a falling liquid film flowing inside a porous medium is an important heat and mass transfer process for absorption chillers and air-conditioners. The presence of air acting as the non-absorbable gas in an absorber is usually unavoidable especially for an open-cycle system. Many studies on the heat and mass transfer for the absorption process have been published [1–10]. Yang and Wood [11] experimentally studied the non-absorbable effects on a wavy film absorption process while Yang and Chen [12] numerically investigated the non-absorbable effects on a smooth film absorption process. The non-absorbable effect on the absorption process taking place on a film flow inside a porous medium has been reported recently only [13].

The mechanism of the non-absorbable gas effect on an absorption process is similar to that of the non-condensable gas effect on a condensation process [14–16]. That is when the absorption of vapor at the liquid–vapor interface drives a continuous vapor flow towards the interface, the non-absorbables are carried along. Since the interface is impermeable to the non-absorbables, they are accumulated near the interface. The partial pressure of vapor at the interface is therefore reduced, and the absorption rate is reduced in turn.

In this study, the absorption process taking place on a falling film flow in a porous medium with the presence of air is considered. Since the equilibrium relations for the absorbent vapor pressure, temperature and concentration are highly non-linear, they make the normalization of the problem difficult. In addition, the study is motivated by the design requirement for an open-cycle absorption solar cooling system [17]. Hence, the physical problem for the aqueous lithium chloride solution and water as the absorbent and refrigerant, respectively, is considered in the present study.

2. Formulation

The problem is formulated corresponding to the coordinate system defined in Fig. 1. A film of aqueous lithium chloride absorbent flowing down in a vertical porous thin film and absorbing the ambient water vapor (refrigerant vapor) with the presence of air acting as the non-absorbable gas is the considered physical model.

---

[*] Corresponding author. Tel.: +886-7525-4222; fax: +886-7525-4299.

E-mail address: yangru@mail.nsysu.edu.tw (R. Yang).

PII: S0017-9310(00)00179-4

Nomenclature

A	surface area
C	LiCl concentration, mass weight percent
C_a	volumetric concentration of non-absorbable gas
$\overline{C_a}$	mass concentration of non-absorbable gas
c_p	specific heat
D	mass diffusivity
Da	Darcy number $= K/H^2$
E	Ergun constant
g	gravitational acceleration
h	heat transfer coefficient
H	film thickness
Ha	heat of absorption
h_m	mass transfer coefficient
R_f	mass transfer coefficient
k	conductivity
K_p	conductivity ratio of solid and fluid
K	permeability
M_{abs}	mass absorption rate per unit width
M_s	liquid mass flow rate
Nu	Nusselt number $= hH/k$
Pr	Prandtl number $= \nu/\alpha$
P_v	absorber pressure
$\overline{P_v}$	normalized pressure $= P_v/P_v^*$
Q	heat transfer rate
Re	Reynolds number $= 4\,\Gamma_0/\nu$
Sh	Sherwood number $= h_m H/D$
T	temperature
u	x-direction velocity
v	y-direction velocity
x	coordinate parallel to the wall
y	coordinate normal to the wall

Greek symbols

α_e	effective thermal diffusivity
Γ_0	mean volumetric flow rate per unit width of the absorber
λ	arbitrary constant for coordinate transformation
ν	kinematic viscosity
ρ	liquid density
ϕ	porosity

Subscripts

a	quantities associated with the air
bulk	bulk mean values
eq	equilibrium condition
in	inlet quantities
out	outlet quantities
s	quantities associated with the solution
w	wall conditions

Superscript

*	reference conditions

The analysis is based on the following assumptions:

1. the liquid is filled (saturated) in the porous medium and the properties of porous medium are assumed to be constant and homogeneous;
2. the liquid properties are assumed to be constant since the variations of temperature and concentration are presumed to be small;
3. the liquid film thickness is assumed constant since the rate of absorbed mass is much less than the mass rate of the main flow;
4. equilibrium of the species exists at the liquid–vapor interface;
5. diffusion is important only in the direction across the film since the Peclet number is practically large;
6. diffusion-thermal effects are negligible [18].

The ambient gas is considered as a uniform flow with a velocity equal to the interface velocity. This consideration is corresponding to a much thicker momentum boundary layer than the concentration and thermal boundary layers wherefore the gas velocity near the gas–liquid interface is nearly uniform and the normal velocity is nearly vanishing.

The governing equation in accordance to these assumptions can be written as follows:

Liquid region: The continue equation is

$$\frac{\partial u}{\partial x} + \frac{\partial v}{\partial y} = 0. \tag{1}$$

The momentum equations can be modeled by the Brinkman–Forchheimer extended Darcy equation since the Reynolds number of fluid flow in the porous medium is greater than 10 [19]. The equations can be written as

$$\begin{aligned} u\frac{\partial u}{\partial x} + v\frac{\partial u}{\partial y} = {} & -\frac{\phi^2}{\rho}\frac{\partial p}{\partial x} + \phi\nu\left(\frac{\partial^2 u}{\partial x^2} + \frac{\partial^2 u}{\partial y^2}\right) \\ & - \phi^2\left(\frac{\nu}{K} + \frac{E}{\sqrt{K}}U\right)u + g\phi^2, \end{aligned} \tag{2}$$

$$\begin{aligned} u\frac{\partial v}{\partial x} + v\frac{\partial v}{\partial y} = {} & -\frac{\phi^2}{\rho}\frac{\partial p}{\partial y} + \phi\nu\left(\frac{\partial^2 v}{\partial x^2} + \frac{\partial^2 v}{\partial y^2}\right) \\ & - \phi^2\left(\frac{\nu}{K} + \frac{E}{\sqrt{K}}U\right)v, \end{aligned} \tag{3}$$

where $U = \sqrt{u^2 + v^2}$ is the Darcian velocity, $E = 1.75\phi^{-3/2}/\sqrt{150}$ is based on Ergun model and $K = d^2\phi^3/150(1-\phi)^2$ is a Kozeny–Carman equation [20].

The heat and mass transfer equations are, respectively,

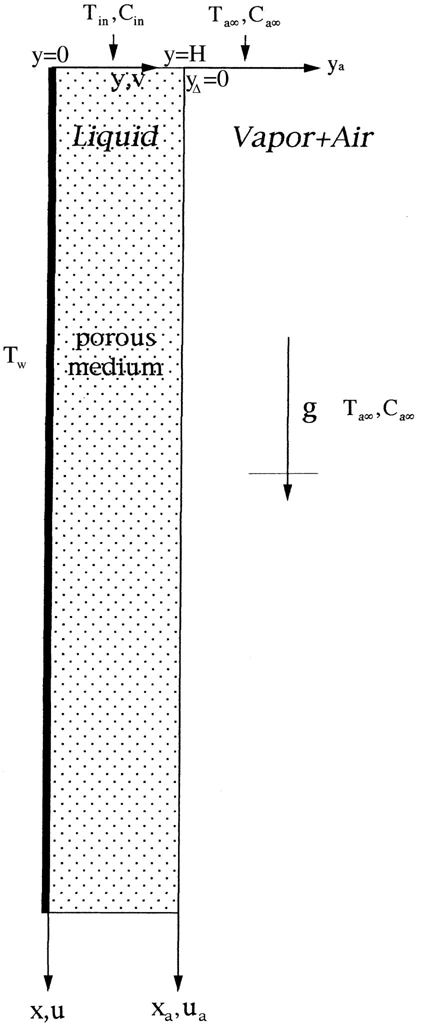

Fig. 1. The coordinate system.

$$u\frac{\partial T}{\partial x}+v\frac{\partial T}{\partial y}=\alpha_{\mathrm{e}}\frac{\partial^2 T}{\partial y^2}, \tag{4}$$

$$\rho u\frac{\partial C}{\partial x}+\rho v\frac{\partial C}{\partial y}=\frac{\partial}{\partial y}\left(\rho D\frac{\partial C}{\partial y}\right), \tag{5}$$

where $\alpha_{\mathrm{e}}=k/\rho_{\mathrm{f}}c_{\mathrm{p_f}}=k_{\mathrm{f}}[\phi+(1-\phi)k_{\mathrm{p}}]/\rho_{\mathrm{f}}c_{\mathrm{p_f}}$ is an effective thermal diffusivity for fluid-saturated porous medium [21].

Gas region: The heat and mass transfer equations for the gas region are, respectively,

$$\rho_{\mathrm{a}}c_{\mathrm{p_a}}u_{\mathrm{a}}\frac{\partial T_{\mathrm{a}}}{\partial x}=\frac{\partial}{\partial y}\left(k_{\mathrm{a}}\frac{\partial T_{\mathrm{a}}}{\partial y}\right), \tag{6}$$

$$\rho_{\mathrm{a}}u_{\mathrm{a}}\frac{\partial \overline{C_{\mathrm{a}}}}{\partial x}=\frac{\partial}{\partial y}\left(\rho_{\mathrm{a}}D_{\mathrm{a}}\frac{\partial \overline{C_{\mathrm{a}}}}{\partial y}\right). \tag{7}$$

Boundary conditions: The suitable boundary conditions for liquid region are

$$1.\ x=0:\quad \begin{aligned}&u=u_{\mathrm{in}},\\&v=0,\\&T=T_{\mathrm{in}},\\&C=C_{\mathrm{in}}.\end{aligned} \tag{8}$$

$$2.\ y=0:\quad \begin{aligned}&u=0,\\&v=0,\\&T=T_{\mathrm{w}},\\&\frac{\partial C}{\partial y}=0.\qquad \text{(non-permeable wall)}\end{aligned} \tag{9}$$

$$3.\ y=H:\quad \begin{aligned}&\frac{\partial u}{\partial y}=0,\\&v=0,\\&-k\frac{\partial T}{\partial y}=\phi\ Ha\ \rho D\frac{\partial C}{\partial y}-k_{\mathrm{a}}\frac{\partial T_{\mathrm{a}}}{\partial y_{\mathrm{a}}}\bigg|_{y_{\mathrm{a}}=0},\\&C=C_{\mathrm{eq}}\left(T|_{y=H},P_{\mathrm{v}}|_{y=H}\right).\end{aligned} \tag{10}$$

The boundary conditions for the gas region are

$$1.\ x=0:\quad \begin{aligned}&T_{\mathrm{a}}=T_{\mathrm{a}\infty},\\&\overline{C_{\mathrm{a}}}=\overline{C_{\mathrm{a}\infty}}.\end{aligned} \tag{11}$$

$$2.\ y_{\mathrm{a}}=0:\quad \begin{aligned}&T_{\mathrm{a}}=T_{y=H},\\&\rho_{\mathrm{a}}D_{\mathrm{a}}\frac{\partial \overline{C_{\mathrm{a}}}}{\partial y_{\mathrm{a}}}=\rho D\frac{\partial C}{\partial y}\bigg|_{y=1}.\end{aligned} \tag{12}$$

$$3.\ y_{\mathrm{a}}=\infty:\quad \begin{aligned}&T_{\mathrm{a}}=T_{\mathrm{a}\infty},\\&\overline{C_{\mathrm{a}}}=\overline{C_{\mathrm{a}\infty}}.\end{aligned} \tag{13}$$

The momentum equation for the liquid region is solved numerically by the SIMPLE algorithm [22]. Since the Peclet number is large in practical applications, the outflow boundary condition is applied at the downstream boundary. The parabolic energy and concentration equations for both liquid and gas regions can be solved by a finite difference method with a marching technique. The boundary conditions of Eq. (13) must be applied far enough from the interface to assure that the boundary layers are within the computational domain. However, for low Reynolds number flows, the appropriate size of y_{a} domain may become very large such that the required number of grids and computation time may become very large. In order to overcome this problem, a coordinate transformation defined by $Y=y_{\mathrm{a}}/(y_{\mathrm{a}}+\lambda)$, where λ is an arbitrary constant, is employed to transform $y_{\mathrm{a}}=\infty$ to $Y=1$, such that the asymptotic ambient conditions can be exactly applied at a finite computational domain. The governing equations (Eqs. (6) and (7)) and the boundary conditions (Eqs. (12) and (13)) are transformed, respectively, into

$$\rho_a c_{p_a} u_a \frac{\partial T_a}{\partial x} = \frac{(1-Y)^2}{\lambda}\frac{\partial}{\partial Y}\left(k_a \frac{(1-Y)^2}{\lambda}\frac{\partial T_a}{\partial Y}\right), \tag{14}$$

$$\rho_a u_a \frac{\partial \overline{C_a}}{\partial x} = \frac{(1-Y)^2}{\lambda}\frac{\partial}{\partial Y}\left(\rho_a D_a \frac{(1-Y)^2}{\lambda}\frac{\partial \overline{C_a}}{\partial Y}\right) \tag{15}$$

and

$$Y = 0: \quad T_a = T_{y=H}, \quad \rho_a D_a \frac{1}{\lambda}\frac{\partial \overline{C_a}}{\partial Y} = \rho D \left.\frac{\partial C}{\partial y}\right|_{y=1}. \tag{16}$$

$$Y = 1: \quad T_a = T_{a\infty}. \tag{17}$$

Since variations of temperature and concentration are expected to be significant in the entrance and interface regions [5,12], the computational grids are chosen to be dense in those regions. A total of 201 points in x, 21 points in y and 201 points in Y are found to be sufficient.

The major concern of an absorption problem is its mass absorption rate that is evaluated by

$$M_{\mathrm{abs}} = M_{\mathrm{sout}} - M_{\mathrm{sin}}. \tag{18}$$

Since the salt is not volatile, its mass flow rate is constant, i.e.,

$$M_{\mathrm{sin}} C_{\mathrm{in}} = M_{\mathrm{sout}} C_{\mathrm{out}}. \tag{19}$$

Eqs. (18) and (19) are combined to obtain

$$M_{\mathrm{abs}} = M_{\mathrm{sin}}\left(\frac{C_{\mathrm{in}}}{C_{\mathrm{out}}} - 1\right). \tag{20}$$

The mass transfer coefficient, h_m, is defined by

$$M_{\mathrm{abs}} = \rho h_m A[C_{\mathrm{in}} - C_{\mathrm{eq}}(T_w, P_v)], \tag{21}$$

where C_{eq} is the concentration when the liquid is in equilibrium with the wall temperature and the ambient vapor pressure. If the wall is sufficiently long, the liquid concentration will approach to C_{eq}; C_{eq} represents the lowest possible concentration of the absorption process.

The heat transfer rate is calculated by performing an energy balance over the entire control volume which results in

$$Q = M_{\mathrm{sin}} h_{\mathrm{sin}} + M_{\mathrm{abs}} H_a - M_{\mathrm{sout}} h_{\mathrm{sout}}. \tag{22}$$

The heat transfer coefficient, h, is defined by

$$Q = hA[T_{\mathrm{eq}}(C_{\mathrm{in}}, P_v) - T_w], \tag{23}$$

where T_{eq} is the temperature when the liquid is in equilibrium with the inlet concentration and the ambient vapor pressure; T_{eq} represents the highest possible temperature of the absorption process.

3. Results and discussion

The base case conditions were chosen as: $C_{\mathrm{in}}^* = 45\%$, $T_{\mathrm{in}}^* = 35°\mathrm{C}$, $T_w^* = 30°\mathrm{C}$, $P_v^* = 1.133$ kPa, $Re^* = 58$, $k_p^* = 10$, $\phi^* = 0.5$ and $C_a^* = 5\%$. The bulk mean temperature and concentration of the solution film are defined, respectively, as

$$T_{\mathrm{bulk}} = \frac{\int_0^H uT\,\mathrm{d}y}{\int_0^H u\,\mathrm{d}y}, \tag{24}$$

$$C_{\mathrm{bulk}} = \frac{\int_0^H uC\,\mathrm{d}y}{\int_0^H u\,\mathrm{d}y}. \tag{25}$$

Then the interface and bulk mean temperatures of the liquid film along the absorber surface are shown in Fig. 2. The interface and the bulk mean concentrations are shown in Fig. 3. The interface temperature is always higher than the bulk mean temperature owing to the heat of absorption released during the absorption pro-

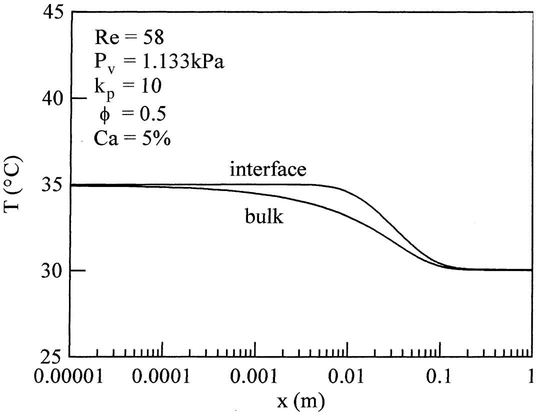

Fig. 2. Typical temperatures of the interface and the bulk mean along the flow direction.

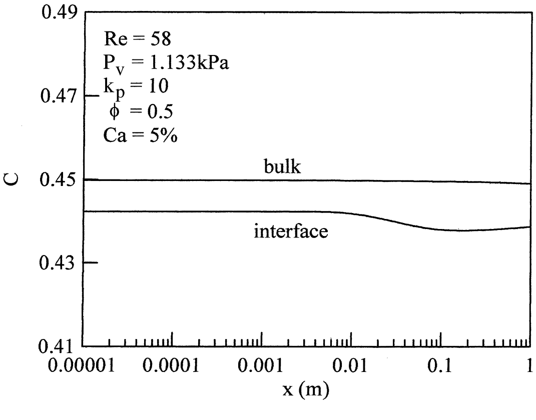

Fig. 3. Typical concentrations of the interface and the bulk mean along the flow direction.

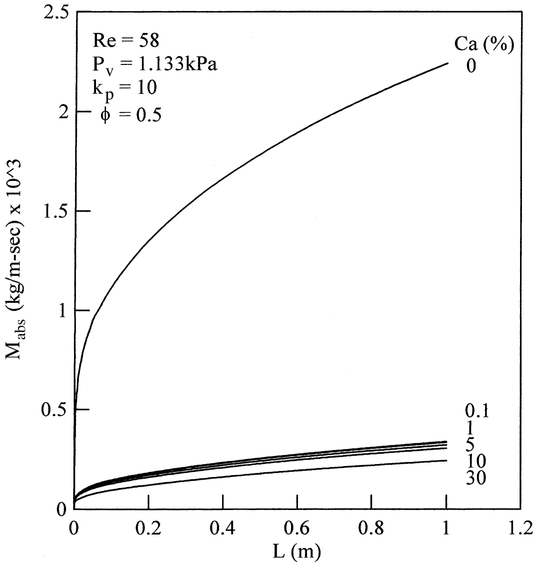

Fig. 4. The effect of non-absorbable gas on the mass absorption rate for various absorber length.

cess taking place on the interface. Both the interface and the bulk mean temperatures drop from the inlet temperature to a value close to wall temperature due to the heat flux into the wall. The interface concentration is much lower than the bulk mean concentration due to the absorption effect on the interface. In addition, the bulk mean concentration decades slowly which confirms that the mass absorption rate is much smaller than the flow rate of the main flow.

The major interest of this study is the effect of the non-absorbable gases on the mass absorption rate. Fig. 4 illustrates that the presence of even a very small amount (e.g. $C_a = 0.1\%$) of non-absorbable gas reduces the absorption rate drastically as compared with the case with no presence of non-absorbables ($C_a = 0\%$). Further increase in non-absorbable content results in further reduction in absorption rate as shown in Fig. 5. A similar plot for decreasing heat transfer rate with increasing non-absorbable content is shown in Fig. 6.

The effect of the absorbent flow rate on the mass absorption rate, M_{abs}, for the cases with $C_a = 5\%$ and $C_a = 10\%$ is shown in Fig. 7. Within the practical application range of *Re* from 30 to 150, the mass absorption flow rate increases almost linearly with increasing flow rate for both cases. The previous solution for wavy film absorption along a smooth surface [14] is also plotted in Fig. 7 for comparison. The main advantage for using porous media is to improve surface wetting for the absorber. Fig. 8 shows the effect of flow rate on the heat transfer rate.

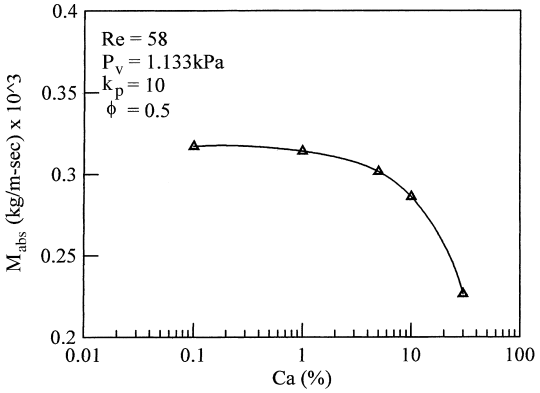

Fig. 5. The effect of non-absorbable gas on the mass absorption rate.

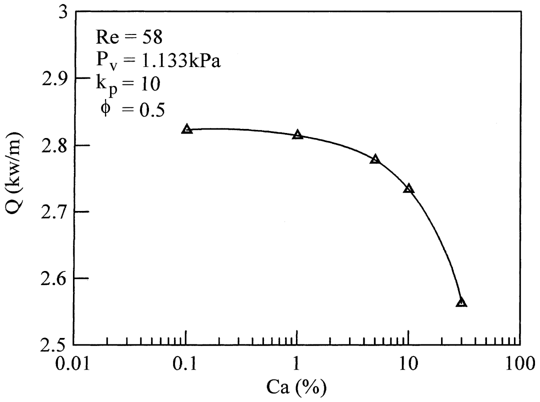

Fig. 6. The effect of non-absorbable gas on the heat transfer rate.

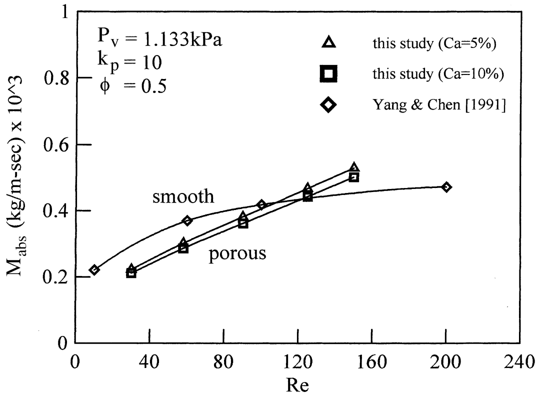

Fig. 7. The effect of the *Re* on the mass absorption rate.

Fig. 9 illustrates the effect of the absorber pressure on the absorption rate for the cases with $C_a = 5\%$ and $C_a = 10\%$. The vapor pressure in the absorber corresponds to the saturation temperature of the evaporator that is the temperature of the chilled water produced by

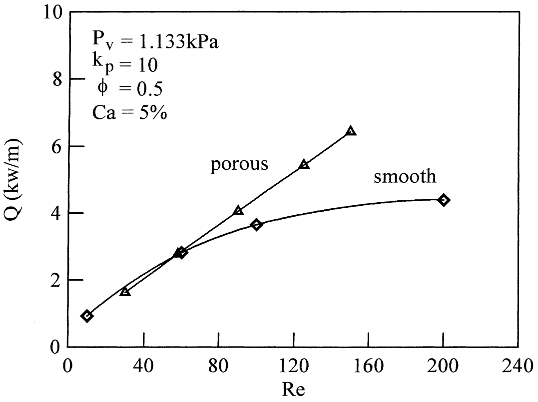

Fig. 8. The effect of the *Re* on the heat transfer rate.

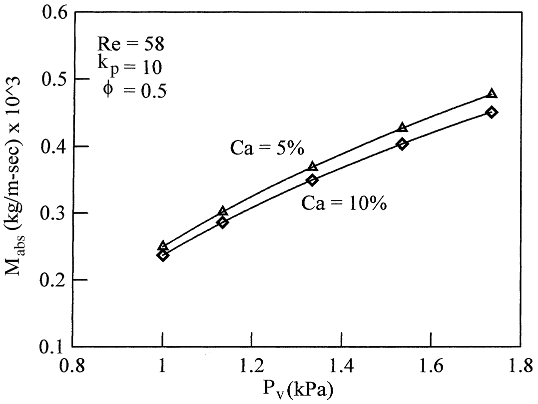

Fig. 9. The effect of the absorber pressure on the mass absorption rate.

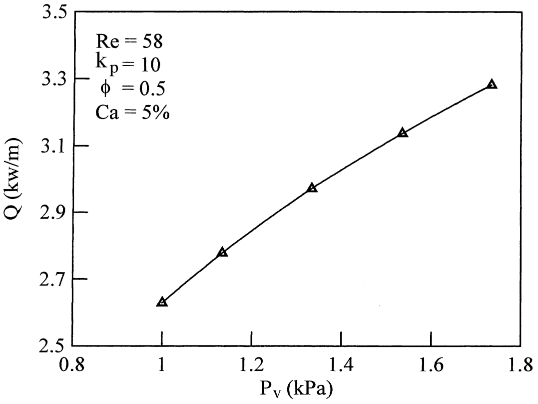

Fig. 10. The effect of the absorber pressure on the heat transfer rate.

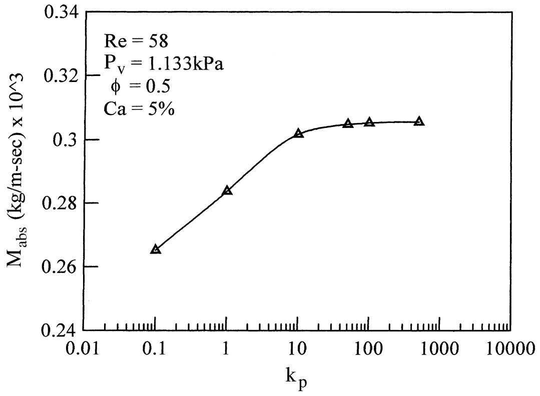

Fig. 11. The effect of conductivity ratio on the mass absorption rate.

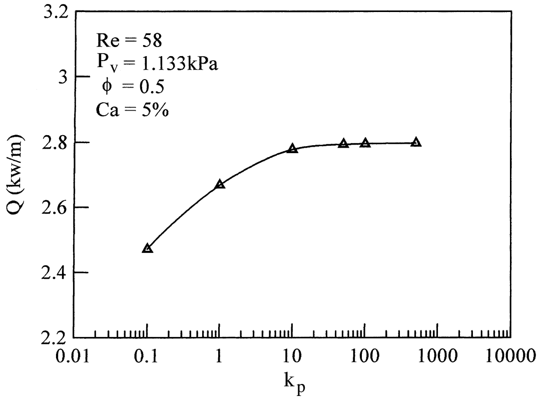

Fig. 12. The effect of conductivity ratio on the heat transfer rate.

the cooling system. The higher the evaporator temperature, the higher the refrigerant vapor pressure. The absorption rate is increased by increasing the driving potential of the vapor pressure difference between the absorber and the solution. Fig. 10 shows a similar increase of the heat transfer rate by the increased vapor pressure.

The effect of conductivity ratio (k_p) on the absorption rate is shown in Fig. 11, from which the absorption rate increases with increased conductivity ratio for $k_p < 10$, further increase in k_p seems to have no effect on the absorption rate. A similar result for heat transfer rate is illustrated in Fig. 12.

Figs. 13 and 14 show the effect of porosity on the absorption rate and the heat transfer rate, respectively. It can be seen that the absorption rate decreases with increasing porosity until $\phi = 0.9$.

In this study, the ranges of the parameters are the flow Reynolds number from 30 to 150, the absorber pressure from 7 to 13 mm Hg, the conductivity ratio from 0.1 to 500, the porosity from 0.5 to 0.95 and the non-absorbable concentration from 0.1% to 30%. The dimensionless heat and mass transfer coefficients are defined, respectively, as

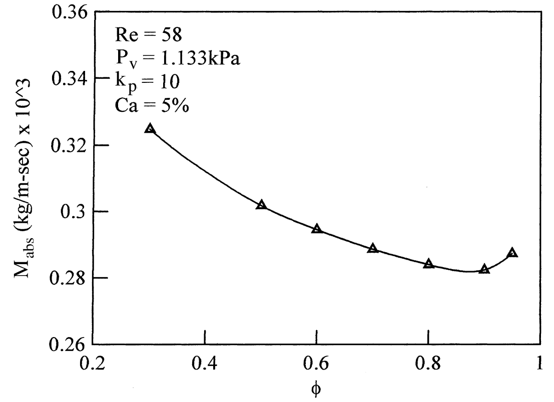

Fig. 13. The effect of porosity on the mass absorption rate.

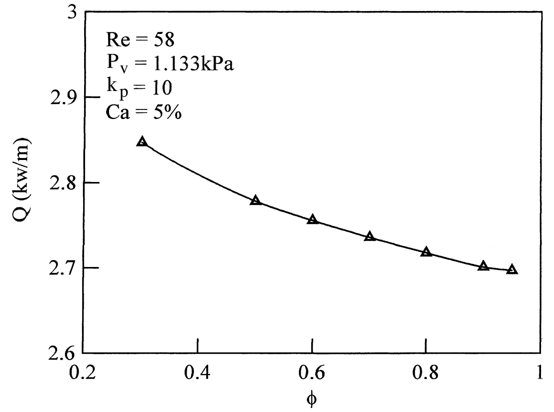

Fig. 14. The effect of porosity on the heat transfer rate.

$$Nu = \frac{hH}{k}, \tag{26}$$

$$Sh = \frac{h_m H}{D}. \tag{27}$$

The following correlations are obtained accordingly as:

$$Nu = 0.00257 Re^{0.865}\ \bar{P}_v^{0.842}\ Da^{-0.005}\ k_p^{0.014} C_a^{-0.011}, \tag{28}$$

$$Sh = 0.0671 Re^{0.563}\ \bar{P}_v^{0.248}\ Da^{-0.01}\ k_p^{0.017} C_a^{-0.04}, \tag{29}$$

for $Re = 30\sim150$, $p_v = 7\sim13$ mm Hg, $C_a = 0.1\sim30\%$, $k_p = 0.1\sim500$ and $\phi = 0.3\sim0.5$.

4. Conclusions

The present study provides an absorber design reference for the non-absorbable gas (air) effect on a falling film absorption process in a porous medium. It is worth noting that the application of porous media in a falling film absorption process is mainly to enhance the wetting conditions, the absorption rate may not be enhanced by using porous media when non-absorbables are present in the absorber. The present results show that the mass absorption rate decreases significantly with increasing absorber air content, but increases with increasing solution flow rate, conductivity ratio and absorber pressure. An optimum conductivity ratio of 10 is observed while a minimum porosity of 0.9 is obtained. The correlations of dimensionless heat and mass transfer coefficients are given for design reference.

Acknowledgements

The authors gratefully acknowledge financial support from the National Science Council, Taiwan, in supporting this research under the contract NSC82-0401-E-110-091.

References

[1] R.E. Emmert, R.L. Pigford, A study of gas absorption in falling liquid films, Chem. Eng. Prog. 50 (2) (1954) 87–93.
[2] S. Banerjee, E. Rhodes, D.S. Scott, Mass transfer to falling wavy liquid films at low Reynolds numbers, Chem. Eng. Sci. 22 (1967) 43–48.
[3] E. Ruckenstein, C. Berbente, Mass transfer to falling liquid films at low Reynolds numbers, Int. J. Heat Mass Transfer 11 (1968) 743–753.
[4] K. Javdani, Mass transfer in wavy liquid films, Chem. Eng. Sci. 29 (1974) 61–69.
[5] G. Grossman, Simultaneous heat and mass transfer in film absorption under laminar flow, Int. J. Heat Mass Transfer 26 (1983) 357–371.
[6] G. Grossman, Heat and mass transfer in film absorption, in: Handbook of Heat and Mass Transfer, Gulf Publishing, New York, 1986.
[7] V.Y.E. Nakoryakov, N.S. Bufetov, N.I. Grigor'yeva, Heat and mass transfer in film absorption, Fluid Mech.-Sov. Res. 11 (1983) 97–115.
[8] H.L. Goff, A. Ramadance, Modeling the coupled heat and mass transfer in a falling film, Proceedings of IHTC-8, Heat Transfer 4 (1986) 1971–1976.
[9] R. Yang, B.D. Wood, A numerical modeling of an absorption process on a liquid falling film, Sol. Energy 48 (3) (1992) 195–198.
[10] R. Yang, D.M. Jou, Heat and mass transfer on the wavy film absorption process, Can. J. Chem. Eng. 71 (1993) 533–538.
[11] R. Yang, B.D. Wood, Experimental study of heat and mass transfer in laminar wavy film absorption with the presence of non-absorbable gases, Chem. Eng. Commun. 125 (1993) 77–90.
[12] R. Yang, J.H. Chen, A numerical study of the non-absorbable effects on the falling liquid film absorption, Waerme- Stoffuebertrag. 26 (1991) 219–223.

[13] R. Yang, D. Jou, Heat and mass transfer of absorption process for the falling film flow inside a porous medium, Int. J. Heat Mass Transfer 38 (1995) 1121–1126.

[14] S. Kotake, Effects of a small amount of noncondensable gas on film condensation of multicomponent mixtures, Int. J. Heat Mass Transfer 28 (1985) 407–414.

[15] C.Y. Wang, C.J. Tu, Effects of non-condensable gas on laminar film condensation in a vertical tube, Int. J. Heat Mass Transfer 31 (1988) 2239–2354.

[16] R. Yang, T.M. Jou, Non-absorbable gas effect on the wavy film absorption process, Int. J. Heat Mass Transfer 41 (1998) 3657–3668.

[17] R. Yang, W.J. Yan, Simulation study for an open-cycle absorption solar cooling system operated in a humid area, Energy 17 (1992) 649–655.

[18] G. Grossman, Analysis of diffusion-thermo effects in film absorption, Proceedings of IHTC-8, Heat Transfer 4 (1986) 1977–1982.

[19] K. Vafai, C.L. Tien, Boundary and inertia effects on convective heat transfer in porous media, Int. J. Heat Mass Transfer 34 (1981) 195–203.

[20] S. Ergun, Fluid flow through packed columns, Chem. Eng. Prog., 1952, pp. 89–94.

[21] A. Bejan, Convection Heat Transfer, Wiley, New York, 1986, p. 353.

[22] S.V. Patankar, Numerical Heat Transfer and Fluid Flow, Hemisphere, Washington, DC, 1980.